Supporting Information

Dual-Emission Fluorescent Silicon Nanoparticles-Based Nanothermometer for Ratiometric Detection of Intracellular Temperature in Living Cells

Jinhua Wang[§], Airui Jiang[§], Jingyang Wang, Bin Song and Yao He**

Laboratory of Nanoscale Biochemical Analysis, Jiangsu Key Laboratory for Carbon-Based Functional Materials and Devices, Institute of Functional Nano & Soft Materials (FUNSOM) and Collaborative Innovation Center of Suzhou Nano Science and Technology (NANO-CIC), Soochow University, Suzhou 215123, China

E-mail: yaohe@suda.edu.cn

E-mail: bsong@suda.edu.cn

1 Experimental method

1.1 Materials and devices

The (3-aminopropyl) trimethoxysilane (97.0%) europium chloride (96.0%), gadolinium chloride (96.0%) and Lyso-tracker Green DND-26 were purchased from Sigma-Aldrich. Trisodium citrate dihydrate (≥ 99.0%) was purchased from Sinopharm Chemical Reagent Co., Ltd (China). Dulbecco's modified eagle media (DMEM), fetal bovine serum; penicillin (100 μg/mL), streptomycin (100 μg/mL) and phosphate buffered saline (PBS) solution were obtained from Invitrogen Corporation (Life Technologies, Shanghai, China). All solutions were prepared using distilled water (Millipore). The microwave system NOVA used for synthesizing materials was made by Preekem of Shanghai, China. The system operated at 2450 MHz frequency and worked at 0-500 W power. Exclusive vitreous vessels with a volume of 50 mL were equipped for the system to provide security during reaction demanding high temperature and pressure. UV-vis absorption spectra were recorded with a Perkin Elmer Lambda 750 UV-vis-near-infrared spectrophotometer. TEM and HRTEM samples were prepared by dispersing the samples onto carbon-coated copper grids with the excess solvent evaporated. The TEM/HRTEM overview images were recorded using Philips CM 200 electron microscope operated at 200 kV. High-resolution X-ray photoelectron spectroscopy (XPS) analyses were performed using a Kratos AXIS Ultra^{DLD} ultrahigh vacuum (UHV) surface analysis system, which consists of a fast entry air lock (base pressure < 1 × 10^{-8} Torr), a multiport carousel chamber (< 5 × 10^{-10} Torr), a deposition chamber (< 5 × 10^{-10} Torr), and an analysis chamber (< 3 ×10^{-10} Torr). A monochromatic Al Kα source (1486.6 eV) with a resolution of 0.1 eV was used to irradiate the samples. XPS samples were prepared by drop-casting Eu@SiNPs (~2 mg) onto aluminum substrates and degassing at 10^{-7} Torr for 15 hours prior to analysis. All XPS spectra were internally calibrated to the C 1s emission (284.8 eV). After calibration, a Shirley-type background was applied to remove most of the extrinsic loss structure. Secondly, to minimize sample charging, the charge neutralizer filament was used when required. FTIR measurements, KBr was pressed into a slice, onto which the Eu@SiNPs sample was dropped. The solvent in the sample was adequately evaporated by irradiation (> 30 min) with a high-power incandescent lamp. FTIR spectra were recorded on a Bruker HYPERION FTIR spectrometer and cumulated 32 scans at a resolution of 4 cm^{-1}. Energy-dispersive X-

ray (EDX) spectroscopy was utilized to determine the fraction of the resultant materials. Laser-scanning confocal fluorescent (Leica, TCS-SP5), equipped with diode laser (405 nm) and multiline argon laser (458, 476, 488, and 514 nm), was used for fluorescent cellular imaging. Images were captured and processed with image analysis software. TGA analysis was performed on a METTLER TOLEDO TGA/STDA 851 instrument. The samples, which ranged in weight from 5 to 12 mg, were placed in a porcelain crucible and heated under air atmosphere from 30 to 800 °C at a rate of 10 °C/min.

1.2 Synthesis of Eu@SiNPs:

The precursor solution was prepared by adding 4 mL of (3-aminopropyl) trimethoxysilane to 16 mL N_2-satureted aqueous solution dispersed with 0.7 g of trisodium citrate. The solution was stirred for 30 min. The resultant precursor solution was transferred into the vitreous vessel with a volume of 50 mL. The precursor solution was heated at 160 ^oC for 30 min under microwave irradiation, and then cooled to ~50 ^oC. Afterwards, europium chloride (from 0.04 to 0.32 mmol) was added to the solution, and then further heated at ~70 ^oC for 20 min under microwave irradiation, producing the Eu@SiNPs. To exclude impurities influence, the (3-aminopropyl) trimethoxysilane molecules, trisodium citrate and europium chloride in solution were removed by dialysis (500 Da). Finally, the Eu@SiNPs with different Eu content (0.25%, 1.0% and 2.0%) were readily achieved. The purified Eu@SiNPs were then used for following characterizations and applications.

1.3 Temperature-dependent measurements:

Fluorescence emission spectra were taken on a Fluorolog-3 Spectrofluorometer (HORIBA Jobin Yvon, Edison, USA). Time-resolved fluorescence decay curves were attained on HORIBA-FM-2015 spectrofluorometer using 370 nm lasers as the excitation source. Steady-state and time-resolved PL spectra at different temperatures were measured with identical test condition. The temperature of the sample in the fluorescence measurement was controlled by a Luma 40^{TM} system (HORIBA Jobin Yvon, USA) with a temperature stability of ±0.1 K. To ensure the thermal equilibration of samples, the time interval of data acquisition is 5 min.

1.4 Synthesis of SiNPs:

Fluorescent SiNPs were readily synthesized through microwave-assisted method based on the previous report. In details, the SiNPs precursor solution was prepared by adding 1 mL (3-aminopropyl) trimethoxysilane to 8 mL N_2-saturated aqueous solution dispersed with 0.075 g trisodium citrate dihydrate. The mixture was stirred for 10 min. The resultant precursor solution was transferred into the exclusive vitreous vessel with a volume of 30 mL. The SiNPs were prepared under 160 °C/120 min. To exclude impurities influence, the residual reagents were removed by dialysis (500 Da). Finally, the purified SiNPs was obtained as a white powder by freeze-drying.

1.5 The MTT assay of cell viability

HeLa (Henrietta Lacks) cells and U87MG (U87MG glioblastoma cancer cells) cells (in H-DMEM medium) were dispersed in 96-well plates (100 μl in each well containing 1×10^4 cells per well). Serial concentrations (0.125, 0.25, 0.5, 1.0 and 2.0 mg/mL) for 3, 6, 12 and 24h (0.125, 0.25, 0.5, 1 and 2 mg/mL) of Eu@SiNPs (with 1.0 % Eu content) solutions as that used in the following cellular imaging were added to each well (10 μL). Incubation was carried out for 3, 6, 12 and 24h in a humidified atmosphere at 37 °C with 5% CO_2. The cytotoxicity of the Eu@SiNPs was evaluated by the MTT (3-(4, 5-dimethylthiazol-2-yl)-2, 5-diphenyltetrazolium bromide) assay (Thiazolyl blue tetrazolium bromide (M5655); Sigma). The assay was based on the accumulation of dark blue formazan crystals inside living cells after exposure to MTT, which is well-established for assessment of cellular viability. The destruction of cell membranes by the addition of sodium dodecylsulfate (SDS) resulted in the liberation and solubilization of the crystals. The number of viable cells was thus directly proportional to the level of the initial formazan product created. The formazan concentration was finally quantified using a spectrophotometer by measuring the absorbance at 570 nm (ELISA reader). A linear relationship between cell number and optical density was established, thus allowing an accurate quantification of changes in the rate of cell proliferation.

1.6 Photoluminescent quantum yields (PLQY) measurements

PLQY, well considered as an important factor for quantitatively evaluating

fluorescent intensity of materials, equals to the ratio of the number of emitted photons and the number of absorbed photons. In our experiment, a well-established reference method was employed for determining the PLQY value of Eu@SiNPs as follow.

$$\Phi_x=\Phi_{st}\,(I_x/I_{st})\,(\eta_x/\eta_{st})^2\,(A_{st}/A_x)$$

Where Φ is the QY, "I" is the integrated emission intensity, "η" is the refractive index of the solvent, and A is the optical density. The subscript "st" and "x" stand for standard with known QY and the Eu@SiNPs sample, respectively. To minimize reabsorption effects, absorption value at the excitation wavelength is required to be smaller than 0.10.[2]

2. Additional data

Fig. S1 shows fast Fourier transform of the Eu@SiNPs.

Fig. S2 shows EDX spectra of the Eu@SiNPs and SiNPs.

Fig. S3 shows FTIR spectra of the Eu@SiNPs and SiNPs.

Fig. S4 shows TGA spectra of the Eu@SiNPs and SiNPs.

Fig. S5 shows solid-state diffuse reflectance spectrum of the SiNPs.

Fig. S6 shows UV-vis spectra of the Eu@SiNPs and SiNPs.

Fig. S7 shows normalized PL spectra of SiNPs at different temperature.

Fig. S8 shows PL spectra of the Eu@SiNPs under continuous UV irradiation for serial times.

Fig. S9 shows radiative and nonradiative recombination rates of the Eu@SiNPs.

Fig. S10 shows the histogram and curve distribution of temperature differences between the obtained from Eu@SiNPs and reference temperatures.

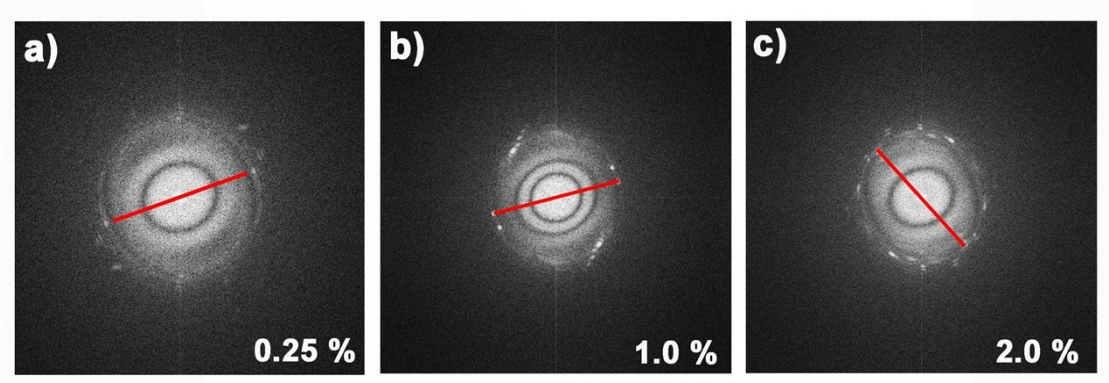

Fig. S1. Fast Fourier transform images of the prepared Eu@SiNPs with different Eu content.

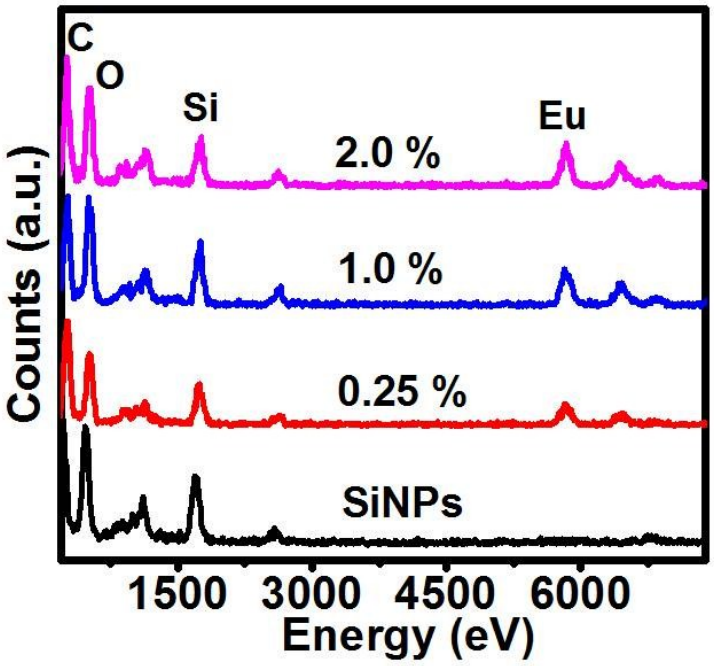

Fig. S2. EDX spectra of the prepared Eu@SiNPs with different Eu content and SiNPs.

To further analyze the chemical compositions of Eu@SiNPs with different Eu content, the EDX analyses were performed. Compare to pure SiNPs only containing Si, C and O elements, the EDX spectra of Eu@SiNPs confirm the presence of Si, C, O and Eu in hybrids system. It is worthwhile to point out that, for EDX measurement, a quantitative analysis of the elemental ratios is not reliable since the supporting substrate is carbon-coated copper girds.[3,4]

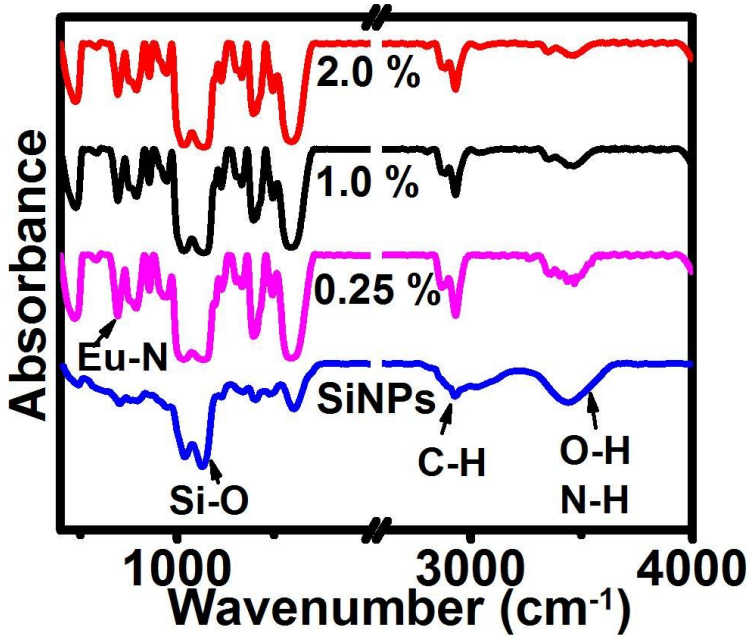

Fig. S3. FTIR spectra of the Eu@SiNPs and SiNPs, exhibiting obvious absorption peaks at 400-4000 cm^{-1}.

The FTIR spectra of the Eu@SiNPs and SiNPs show characteristic absorption bands for N-H and O-H stretching vibrations of the amino and hydroxyl groups near 3100 and 3300 cm^{-1}. Two signals at 1010 and 1090 cm^{-1} are ascribed to Si-O-Si and Si-O-C vibrations, respectively. The strong absorbance at 1390-1440 and 1580 cm^{-1} are, respectively, assigned to the C-O and N-H bending vibrations. The signals at 600-700 cm^{-1} of Eu@SiNPs are ascribed to Eu-N vibrations.[1,5]

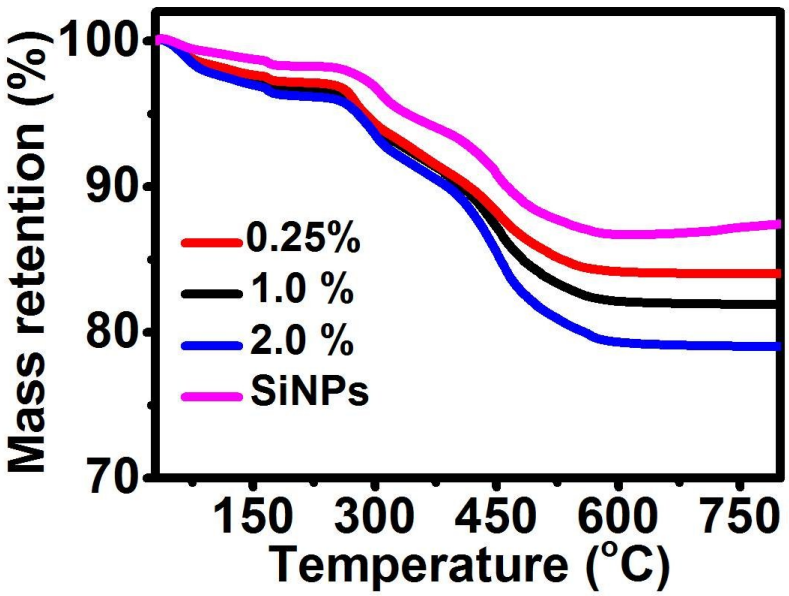

Fig. S4. TGA spectra of Eu@SiNPs with different Eu content and SiNPs.

Fig. S4 gives the TGA thermograms of Eu@SiNPs and SiNPs under air from room temperature to 800 °C. Rapid mass loss between 150 and 480 °C is observed for as-prepared samples, which is ascribed to the burning of carbonous residues. Comparatively, the as-prepared samples exhibit a weight increase above 600 °C resulted from Si oxidation ($Si + O_2 \rightarrow SiO_2$). At 800 °C, the residual weight percentage is 83.9 % for 0.25% Eu content, 81.8 % for 1.0 % Eu content, 79.0 % for 2.0 % Eu content, and 87.5 % for SiNPs.[6] These results suggest that the Eu@SiNPs obtained from higher concentration of Eu yield greater weight losses.

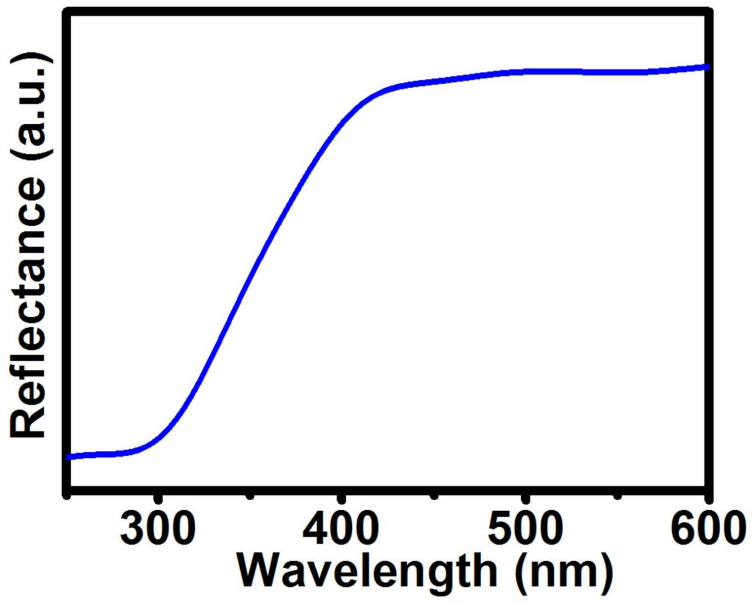

Fig. S5. Solid-state diffuse reflectance spectrum of the SiNPs.

The SiNPs show an absorption band at 300 nm in the UV region of its diffuse reflectance spectrum, which is assigned to the $\pi \rightarrow \pi^*$ transition of the ligand. The observed band in the UV region of diffuse reflectance spectrum SiNPs is thought to correspond to electronic transitions from the ground state level S_0 to the excited state level S_1.[7]

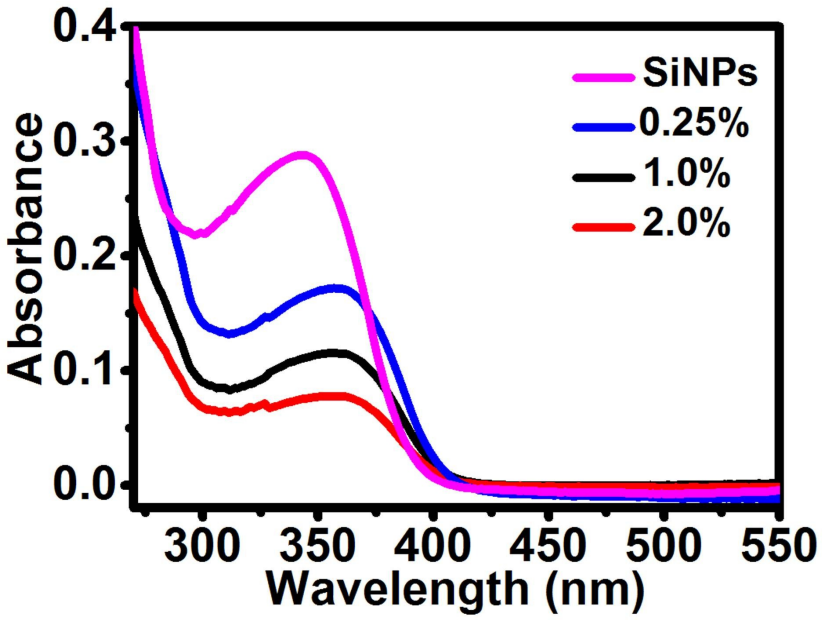

Fig. S6. UV-vis spectra of SiNPs and Eu@SiNPs with different Eu content.

The SiNPs show a strong absorption from 300 to 360 nm (peak is centered at 350 nm). The Eu@SiNPs with different Eu content also display strong wide absorption peaks at 360 nm, implying that the Eu ions are coordinated with the groups of SiNPs and the fluorescence emission of the Eu is mainly sensitized by the absorption of the SiNPs.[8]

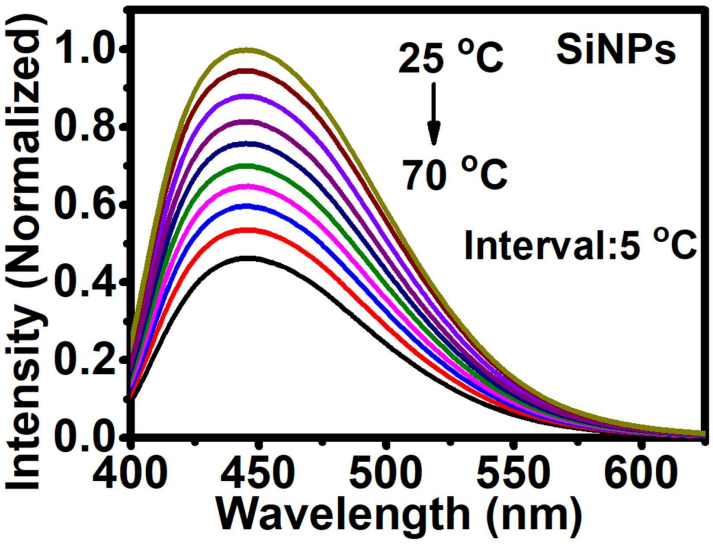

Fig. S7. Normalized PL spectra of SiNPs at different temperature.

Fig. S7 shows the temperature dependence of the PL spectra of the SiNPs. The intensity at 455 nm distinctly decreases upon raising the temperature from 25 to 70 ^{o}C without spectral shifts in the investigated temperature window.

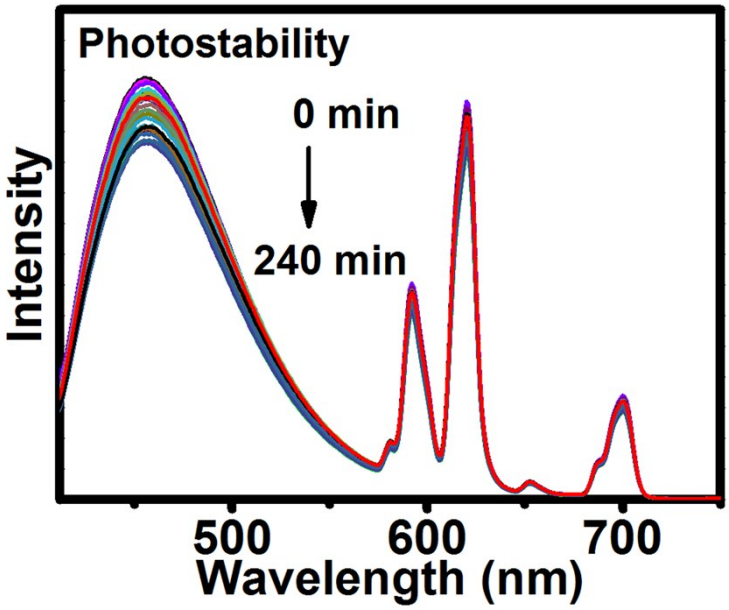

Fig. S8. PL spectra of aqueous solutions of Eu@SiNPs under continuous UV irradiation for serial times.

Both blue emission (at 455 nm) and red emission (at 620 nm) of Eu@SiNPs are highly photostable, preserving ~89 and ~95% of the initial fluorescent intensities after 4-h treatment, respectively.

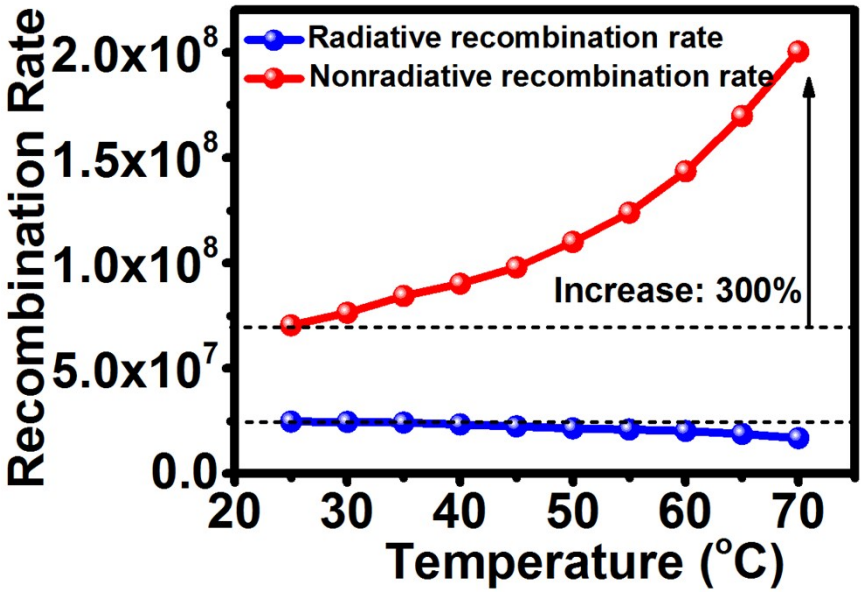

Fig. S9. Radiative (blue symbols) and nonradiative (red symbols) recombination rates for Eu@SiNPs plotted against the temperature for temperatures of 25-70 °C.

The radiative recombination rate is lower than the correspondent nonradiative rate and remains stable at temperatures between 25 and 70 °C. However, there is a sharp increase in the rate of nonradiative recombination when increasing the temperature range. These results demonstrate that the temperature-dependent PL property in Eu@SiNPs is primarily caused by the activation of nonradiative relaxation channels.

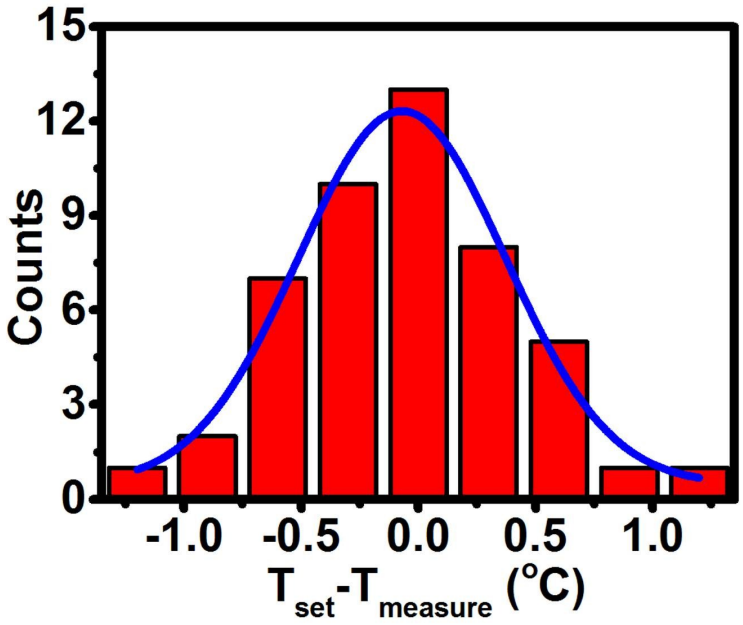

Fig. S10. Histogram distribution of temperature differences between the obtained and reference temperatures; the solid line is the distribution curve.

As shown in Fig. S10, the absolute average accuracy of temperature detection by the presented method is calculated to be 0.25 °C. This experiment confirms the potential feasibility of Eu@SiNPs-based thermal probes in biological systems.[9]

References

(1) Y. L. Zhong, F. Peng, F. Bao, S. Y. Wang, X. Y. Ji, L. Yang, Y. Y. Su, S. T. Lee, Y. He, *J. Am. Chem. Soc.* 2013, **135**, 8350-8356.

(2) H. Qin, Y. Niu, R. Meng, X. Lin, R. Lai, W. Fang, X. Peng, *J. Am. Chem. Soc.* 2014, **136**, 179-187.

(3) T. K. Purkait, M. Iqbal, M. H. Wahl, K. Gottschling, C. M. Gonzalez, M. A. Islam, J. G. C. Veinot, *J. Am. Chem. Soc.* 2014, **136**, 17914-17917.

(4) J. D. Holmes, K. J. Ziegler, R. C. Doty, L. E. Pell, K. P. Johnston, B. A. Korgel, *J. Am. Chem. Soc.* 2001, **123**, 3743-3748.

(5) X. Li, Y. Xie, B. Song, H. L. Zhang, H. Chen, H. Cai, W. Liu, Y. Tang, *Angew. Chem. Int. Ed.* 2017, **56**, 2689-2693.

(6) Y. S. Jung, K. T. Lee, S. M. Oh, *Electrochimica Acta.* 2007, **52**, 7061-7067.

(7) Y. Zhou, X. Li, L. Zhang, Y. Guo, Z. Shi, *Inorg. Chem.* 2014, **53**, 3362-3370.

(8) B. Chen, J. Feng, *J. Phys. Chem. C* 2015, **119**, 7865-7872.

(9) O. S. Wolfbeis, *Chem. Soc. Rev.* 2015, **44**, 4743-4768.